Published OnlineFirst August 1, 2011; DOI: 10.1158/1541-7786.MCR-10-0474

Cell Cycle, Cell Death, and Senescence

Molecular Cancer Research

Forced Activation of β-Catenin Signaling Supports the Transformation of *hTERT*-Immortalized Human Fetal Hepatocytes

Henning Wege[1], Denise Heim[1], Marc Lütgehetmann[1], Judith Dierlamm[2], Ansgar W. Lohse[1], and Tim H. Brümmendorf[3]

Abstract

Hepatocarcinogenesis is a multistep process driving the progressive transformation of normal liver cells into highly malignant derivatives. Unlimited proliferation and telomere maintenance have been recognized as prerequisites for the development of liver cancer. Moreover, recent studies identified illegitimate β-catenin signaling as relevant hit in a considerable subset of patients. To further investigate the currently not well-understood malignant evolution driven by telomerase and β-catenin, we monitored cytogenetic and phenotypic alterations in untransformed telomerase-immortalized human fetal hepatocytes following forced activation of β-catenin signaling. As expected, constitutive activation of β-catenin signaling significantly enhanced proliferation with decreasing serum dependence. Previously intact contact inhibition was almost completely eliminated. Interestingly, after several passages in cell culture, immortalized clones with dominant-positive β-catenin signaling acquired additional chromosomal aberrations, in particular translocations, anchorage-independent growth capabilities, and formed tumors in athymic nude mice. In further support for the driving role of β-catenin during hepatocarcinogenesis, improved colony growth in soft agar and accelerated tumor formation was also confirmed in Huh7 cells following stable expression of the constitutively active S33Y β-catenin mutant. Telomerase inhibition showed that short-term expansion of transformed clones was not telomerase dependent. Finally, cancer pathway profiling in derived tumors revealed upregulation of characteristic genes associated with invasion and angiogenesis. In conclusion, illegitimate activation of β-catenin signaling enhances the transformation from immortalization to malignant growth in human fetal hepatocytes. Our data functionally confirm a permissive role for β-catenin signaling in the initial phase of hepatocarcinogenesis. *Mol Cancer Res; 9(9); 1222–31.* ©*2011 AACR.*

Introduction

Hepatocellular carcinoma is the third leading cause of cancer mortality worldwide with continuously rising incidence rates in Western countries (1, 2). Although the principal clinical risk factors for hepatocellular carcinoma are well defined, molecular mechanisms contributing to tumor initiation and early progression are still not completely understood. In almost 90% of human malignancies, telomerase activation, characteristically mediated by reexpression of the rate-limiting catalytic subunit human telomerase reverse transcriptase (*hTERT*), has been observed as early event (3). Telomerase is a cellular RNA–dependent DNA polymerase responsible for telomere maintenance and stabilization (4). Telomeres are protective nucleoprotein structures at the end of linear chromosomes (5). In normal somatic cells, *hTERT* is suppressed and consequently telomerase is not active. Because of the end replication problem, telomeres progressively shorten with every cell division until a critical length is reached and the cells enter senescence, a postmitotic quiescent state (6). Interestingly, several studies have recently showed telomerase activation already in precancerous hepatic lesions (7–10). On the basis of these findings, telomerase activation has been proposed as an early prerequisite in hepatocarcinogenesis (11, 12). In addition to a limitless replicative potential (immortalization), further genetic alterations are required for self-sufficiency in growth signals, insensitivity to antigrowth signals, effective evasion of apoptosis, and altered differentiation (13).

In a considerable subset of patients with hepatocellular carcinoma, Wnt/β-catenin signaling is activated (14). This pathway is, for example, crucial for the expansion

Authors' Affiliations: Departments of [1]Gastroenterology and Hepatology and [2]Hematology and Oncology, University Medical Center Hamburg-Eppendorf, Hamburg; and [3]Department of Hematology and Oncology, University Medical Center Aachen, Aachen, Germany

Note: Supplementary data for this article are available at Molecular Cancer Research Online (http://mcr.aacrjournals.org/).

Corresponding Author: Henning Wege, University Medical Center Hamburg-Eppendorf, Martinistr. 52, D-20246 Hamburg, Germany. Phone: 49-40-7410-52495; Fax: 49-40-7410-59092; E-mail: hwege@uke.de

doi: 10.1158/1541-7786.MCR-10-0474

Published OnlineFirst August 1, 2011; DOI: 10.1158/1541-7786.MCR-10-0474

and survival of embryonic hepatoblasts (15, 16). Recently, animal models also revealed that mobilization of hepatic stem cells during liver regeneration is associated with activation of Wnt/β-catenin signaling (17, 18). β-Catenin is the key signaling molecule of the pathway. In the absence of activating ligands, a destruction complex consisting of axin, adenomatous polyposis coli (APC) protein, and glycogen synthase kinase-3β (GSK-3β), phosphorylates β-catenin in the cytoplasm. Phosphorylated β-catenin undergoes degradation. In the activated state, Wnt binds to the membrane receptor frizzled and induces the dissociation of the destruction complex. β-Catenin escapes degradation and accumulates in the cytoplasm leading to increased translocation into the nucleus, where β-catenin initiates the expression of various target genes (17, 19, 20). Activation of Wnt/β-catenin signaling, primarily caused by inactivating mutations in *APC*, *AXIN1*, or *CTNNB1* (21, 22), has recently been identified as a permissive pathway driving downstream transformation events in colorectal cancer (23). Interestingly, compared with the subgroup with *TP53* mutations, liver cancers with activating mutations in *CTNNB1* have relatively little chromosomal instability (24), suggesting a driving role for this pathway also in hepatocarcinogenesis.

In this study, we employed previously characterized telomerase-immortalized human fetal hepatocytes (FH-hTERT) as cell culture model for untransformed proliferating human liver cells (25, 26). To analyze the functional consequences of an aberrantly activated β-catenin–related transcription (CRT), we monitored cancer cell characteristics and transformation events in FH-hTERT following forced activation of β-catenin signaling.

Materials and Methods

Cell lines and plasmids

The local ethics committee approved utilization of FH-hTERT cells (approval number OB-034/06). FH-hTERT clones were used at population doubling (PD) 35 to 40 (just bypassing the senescence checkpoint) and 80 to 100. As described before, FH-hTERT did not display a malignant phenotype (25). As control human liver cancer cell lines, we cultured β-catenin–positive HepG2 and a Huh7 clone with a low baseline β-catenin expression (Supplementary Fig. S1). Expression vectors for the wild-type and the constitutively active S33Y β-catenin mutant (pbcatwt and pbcatS33Y, respectively) were kindly provided by H. Clevers (Hubrecht Laboratory, Utrecht, Netherlands). The backbone vector pcDNA (Invitrogen) was transfected as vector control.

Cell culture and transfection

All cells were cultured in Dulbecco's Modified Eagle Medium with high glucose (4.5 g/L), 10% inactivated FBS, and antibiotics (Invitrogen). For FH-hTERT, culture medium was additionally supplemented with 5 μg/mL insulin and 2.4 μg/mL hydrocortisone (Sigma-Aldrich). Cells were nucleofected using Nucleofector Solution V (Amaxa) and program T30 and subsequently selected with Zeocin (Invitrogen) at 200 μg/mL for FH-hTERT and 50 μg/mL for Huh7 cells.

Plasmid expression analysis and immunoblot

To quantitate β-catenin expression, RNA was extracted with RNeasy Mini Kit (Qiagen) and reverse transcribed with ThermoScript RT-PCR Systems (Invitrogen). For real-time quantitative PCR (qPCR), we employed a validated primer set for *CTNNB1* together with various internal reference genes (*GAPDH*, *RPL13A*, *B2M*, *TBP*) as basket housekeeper (QuantiTect Primer Assay; Qiagen). Amplification was carried out with QuantiTect SYBR Green PCR Master Mix (Qiagen) on an ABI Prism 7900H thermal cycler (Applied Biosystems). PCR efficiency (E) was determined for each amplicon. Finally, expression levels were derived by an efficiency-corrected model and comparative quantification, $E^{\Delta C_t[CTNNB1]}/E^{\Delta C_t[\text{reference genes}]}$, (27). In addition, cell lysates were extracted and quantified with the BCA Protein Assay Kit (Pierce Biotechnology). SDS-PAGE was conducted with 20 μg protein per lane. Following blotting, nitrocellulose membranes were blocked with 5% nonfat dry milk. Primary antibody solution detecting β-catenin (1:200; Santa Cruz Biotechnology) was incubated at 4°C overnight. Incubation with species-specific secondary antibody solution (1:1,000; Santa Cruz Biotechnology) conjugated with horseradish peroxidase was carried out for 45 minutes at room temperature. Detection was achieved with the ECL Western Blotting Analysis System (Amersham Biosciences).

Dual-luciferase reporter assay

CRT reporter plasmids (Super8XTOPFlash and Super8-XFOPFlash) were kindly provided by R.T. Moon (Howard Hughes Medical Institute, Seattle, WA). The TOPFlash plasmid (M50) contains T-cell factor/lymphoid enhancing factor (TCF/LEF)-binding sites driving the expression of *Firefly* luciferase. The control plasmid FOPFlash (M51) carries mutant TCF/LEF-binding sites. As coreporter vector, pRL-CMV with cytomegalovirus (CMV)-driven expression of *Renilla* luciferase (Promega) was used to monitor transfection efficiency. Cells were transfected by lipofection with JetPEI (Polyplus) according to instructions from the manufacturer. Two days after transfection, cells were harvested and assayed using the Dual-Luciferase Reporter Assay System (Promega). CRT was expressed as luciferase activity ratio M50/M51, following correction for transfection efficiency (M50/pRL-CMV and M51/pRL-CMV).

Cell proliferation tests

To monitor cell proliferation, we conducted serial cell counts in a standard hemocytometer. In addition, we employed the CellTiter 96 AQueous One Solution Cell Proliferation Assay (Promega) seeding 5×10^3 cells per well in 96-well plates. At each time point, an entire column ($n = 8$) was assayed and the mean optical density (OD)

Published OnlineFirst August 1, 2011; DOI: 10.1158/1541-7786.MCR-10-0474

value was calculated. ΔOD was obtained by comparing the reading with the mean OD obtained 12 hours after seeding.

Serum dependence and contact inhibition

To investigate serum dependence, cells were seeded in 96-well plates and serum was omitted in the following medium changes. Proliferation was monitored as described above. Cell-cycle profiles of near-confluent (40% to 60%) and superconfluent cultures (culture for 3 days after reaching confluency as determined by phase contrast microscopy) were obtained by incubating fixed cells in propidium iodide solution (working concentration 25 μg/mL) containing RNase A (500 U/mL) at 37°C for 30 minutes before evaluation on a FACSCanto flow cytometer (Becton Dickinson). Cell-cycle distribution of cells was determined using ModFit (Verity Software House).

Cytogenetic investigations

Multicolor karyotyping FISH (mFISH) was conducted using the 24XCyte Color Kit for human chromosomes (MetaSystems) according to the supplier's recommendations and as previously described (25). We employed the Genome-Wide Human SNP Array 6.0 and the Genotyping Console Software 4.0 (Affymetrix) to assess microamplifications and deletions in DNA samples obtained from transformed cells in comparison to the HapMap reference (Affymetrix) and untransformed counterparts. Array analyses were conducted in the Array Service Center of the Department of Clinical Chemistry, University Medical Center Hamburg-Eppendorf.

Anchorage-independent growth

Soft agar colony assays were conducted as previously summarized (26).

Tumor formation in nude mice

Animal experimentation was approved by the local review board (protocol number 25/06). All animals received humane care. Tumorigenicity was assessed by inoculating 2×10^6 cells in 100 μL culture medium with 2% serum and mixed with 100 μL Matrigel (Sigma-Aldrich) subcutaneously into the dorsal flanks of 8- to 12-week-old NMRI athymic nude mice (Animal Facility, University Medical Center Hamburg-Eppendorf). Tumor formation was observed for a minimum of 12 months and measured 3 times per week using a caliper. Tumor volume was estimated as $(D^2 \times d)/2$, where D is the large diameter and d the smaller diameter of the tumor.

Tumor genotyping

For genotyping, tumor DNA was extracted with DNeasy Blood and Tissue Kit (Qiagen). Amplification of specific sequences of the selection markers enclosed in the 2 expression plasmids introduced in our cell clones [puromycin *N*-acetyltransferase (*PAC*) and Zeocin resistance gene (*SH ble*)] was conducted using Platinum PCR SuperMix (Invitrogen). Primer sequences are as follows: β-actin (*ACTB*): GGC ATC CTC ACC CTG AAG TA and GTC AGG CAG CTC GTA GCT CT, *PAC*: ACC GAG CTG CAA GAA CTC TTC CTC and CCA GGA GGC CTT CCA TCT GTT G, and *SH ble*: GGA CTT CGT GGA GGA CGA C and CAC GAC CTC CGA CCA CTC. In addition to tumor samples, DNA from Huh7 (negative control), FH-hTERT (*PAC* =positive control), FH-hTERT pbcatS33Y (*SH ble* positive control), and mouse liver cells (background control) were analyzed.

Immunofluorescence of tumor samples

To visualize human cells within the observed tumors, cryostat sections were immunostained with a human-specific antibody recognizing the nuclear antigen SP-100 (kindly provided by H. Will, Heinrich-Pette-Institute, Hamburg, Germany). Sections were fixed in acetone for 10 minutes. After blocking sections in 1% bovine serum albumin solved in Tris-buffered saline (pH = 7.5) with 0.05% Tween-20 for 1 hour, the primary antibody was applied with a dilution of 1:400 for 1 hour. A species-specific fluorescence-labeled secondary antibody (Alexa-Fluor 488; Invitrogen) was employed for visualization. Finally, sections were counterstained with 4′,6-diamidino-2-phenylindole (DAPI) and examined under a fluorescence microscope.

Telomerase inhibition

RNA interference (RNAi) was utilized to suppress telomerase function. Via nucleofection (Nucleofector Solution V, program T30) an siRNA corresponding to the essential RNA component of the human telomerase holoenzyme (hTERC; sc-106994; Santa Cruz Biotechnology) was introduced to knockdown *hTERC* expression and telomerase activity. To inhibit potential noncanonical hTERT functions, *hTERT* expression was targeted employing a small hairpin RNA (shRNA; sc-156050-SH; Santa Cruz Biotechnology) and lipofection. A lipofection protocol was required to knockdown *hTERT*, as nucleofection induced *hTERT* transcription. Expression of *hTERC* and *hTERT* were determined 48 hours following transfection. For the qPCR protocol described above, a validated primer set for *hTERT* (sc-156050-PR; Santa Cruz Biotechnology), a self-designed and optimized primer set for *hTERC* (GCCTTCCACCGTTCATTCTA and GGCZGACAGAGCCCAACTC) and the basket housekeeper were used. Telomerase activity in extracts from 1,000 cells was measured and expressed as relative telomerase activity (RTA) in comparison with telomerase-positive 293T cells with the real-time quantitative telomeric repeat amplification protocol (RQ-TRAP) as outlined before (28).

Cancer pathway profiling

DNase-treated RNA from FH-hTERT pcDNA, FH-hTERT pbcatS33Y, and 4 independent tumor samples, extracted with RNeasy Mini Kit (Qiagen), were reverse transcribed with ThermoScript RT-PCR Systems (Invitrogen). After diluting the cDNA synthesis reaction with ddH_2O (1:5.55), expression profiling was conducted with the RT^2 Profiler PCR Array System (SABiosciences) on an

Published OnlineFirst August 1, 2011; DOI: 10.1158/1541-7786.MCR-10-0474

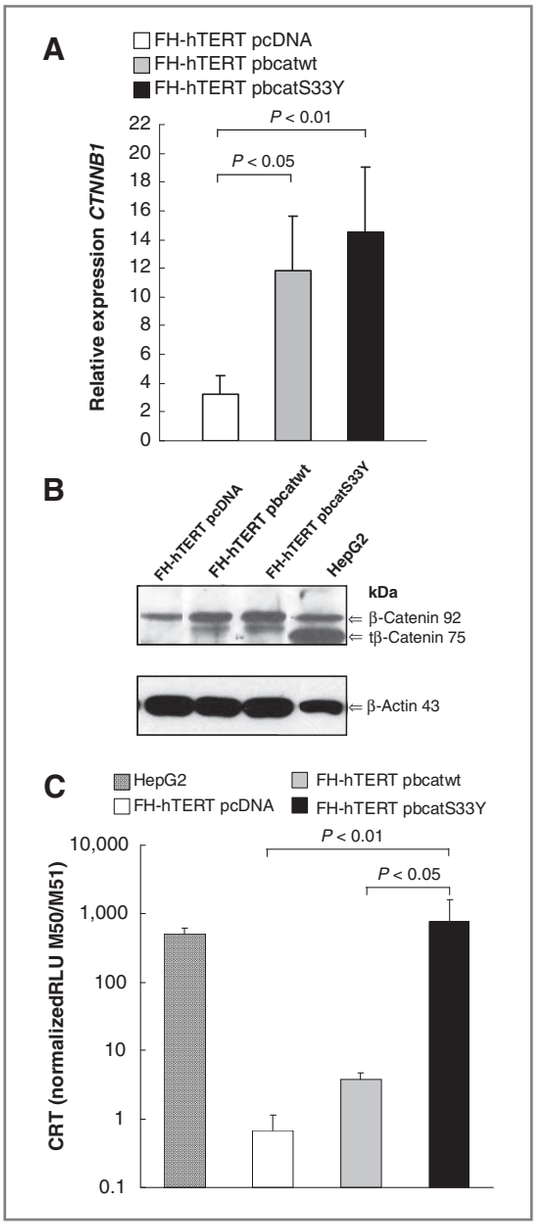

Figure 1. Constitutive β-catenin activation. A, relative expression levels of β-catenin were determined by qPCR with a basket housekeeper as internal control and 1 FH-hTERT pcDNA sample as calibrator (expression level = 1). Bar graphs represent average expression levels (SD = error bars). B, accumulation of β-catenin was evaluated by immunoblotting. HepG2 cells served as a positive control (typical additional truncated 75 kDa β-catenin band) and β-actin was visualized as a loading control. C, a dual-luciferase reporter assay was conducted to determine CRT. HepG2 cells were assayed as a positive control. Bar graphs (SD = error bars) represent average CRT, expressed as luciferase activity ratio M50/M51 following correction for transfection efficiency. RLU, relative luciferase units.

ABI Prism 7900H thermal cycler (Applied Biosystems). Primer sets on the array represent biological pathways involved in transformation and tumorigenesis. In addition, the panel includes a set of reference genes as well as RNA and qPCR quality controls. Expression levels were determined by comparative quantification [$2^{(-\Delta\Delta C_T)}$] employing FH-hTERT pcDNA as calibrator (expression level = 1).

Statistical analysis

All experiments were carried out in triplicates and with 2 to 3 repetitions. Data are presented as mean ± SD. The unpaired Student's *t* test was used for statistical analysis and values of $P < 0.05$ were considered statistically significant.

Results

Expression of dominant-positive β-catenin

FH-hTERT display low Wnt/β-catenin pathway activity as determined with a dual-luciferase reporter assay measuring β-catenin–regulated gene expression (CRT). Incubation with 40 mmol/L LiCl, a GSK-3β inhibitor and chemical pathway activator, transiently enhanced CRT and showed the possibility to activate β-catenin signaling in our cell clones (data not shown). Transfection of FH-hTERT with the constitutively active S33Y β-catenin mutant (pbcatS33Y) as well as with the wild-type control (pbcatwt) resulted in a significant increase in β-catenin transcripts determined by qPCR (Fig. 1A). Following selection and expansion of Zeocin-resistant cells, increased protein levels of β-catenin were observed in cells transfected with either of the 2 β-catenin expression plasmids. In comparison, only a faint β-catenin band was observed in FH-hTERT transfected with pcDNA (Fig. 1B). In FH-hTERT stably transfected with pbcatS33Y (FH-hTERT pbcatS33Y), increased β-catenin levels resulted in a robust upregulation in downstream pathway activity (Fig. 1C). CRT levels were not substantially increased in FH-hTERT pbcatwt because the wild-type β-catenin is not translocated into the nucleus and does therefore not lead to target gene activation.

Forced β-catenin activation induces cancer cell stigmata

To functionally characterize phenotype alterations induced by forced β-catenin activation, we monitored proliferation, serum dependence, and contact inhibition. In comparison with FH-hTERT pbcatwt, forced β-catenin activation (FH-hTERT pbcatS33Y) resulted in an accelerated cellular growth. This was confirmed by serial cell counts (Fig. 2A) and a photometric assay monitoring proliferation more closely (Fig. 2B). We also cultured the clones with 2% serum. Three days after seeding, we detected a significant difference in cell density between FH-hTERT pbcatS33Y and FH-hTERT pbcatwt. This difference reflects the accelerated growth in FH-hTERT pbcatS33Y (see above). However, serum-free culture significantly reduced cellular growth in FH-hTERT pbcatwt (Fig. 2C), with a 20% reduction in cell density compared with cells cultured with 2% serum for 3 days. In contrast, serum depletion did not significantly affect cellular growth in FH-hTERT pbcatS33Y (Fig. 2C). To determine changes in contact inhibition, we compared S-phase fractions in confluent cultures (3 days after reaching 100% confluency) with log-proliferating cultures (40% to 60% confluency). In

Published OnlineFirst August 1, 2011; DOI: 10.1158/1541-7786.MCR-10-0474

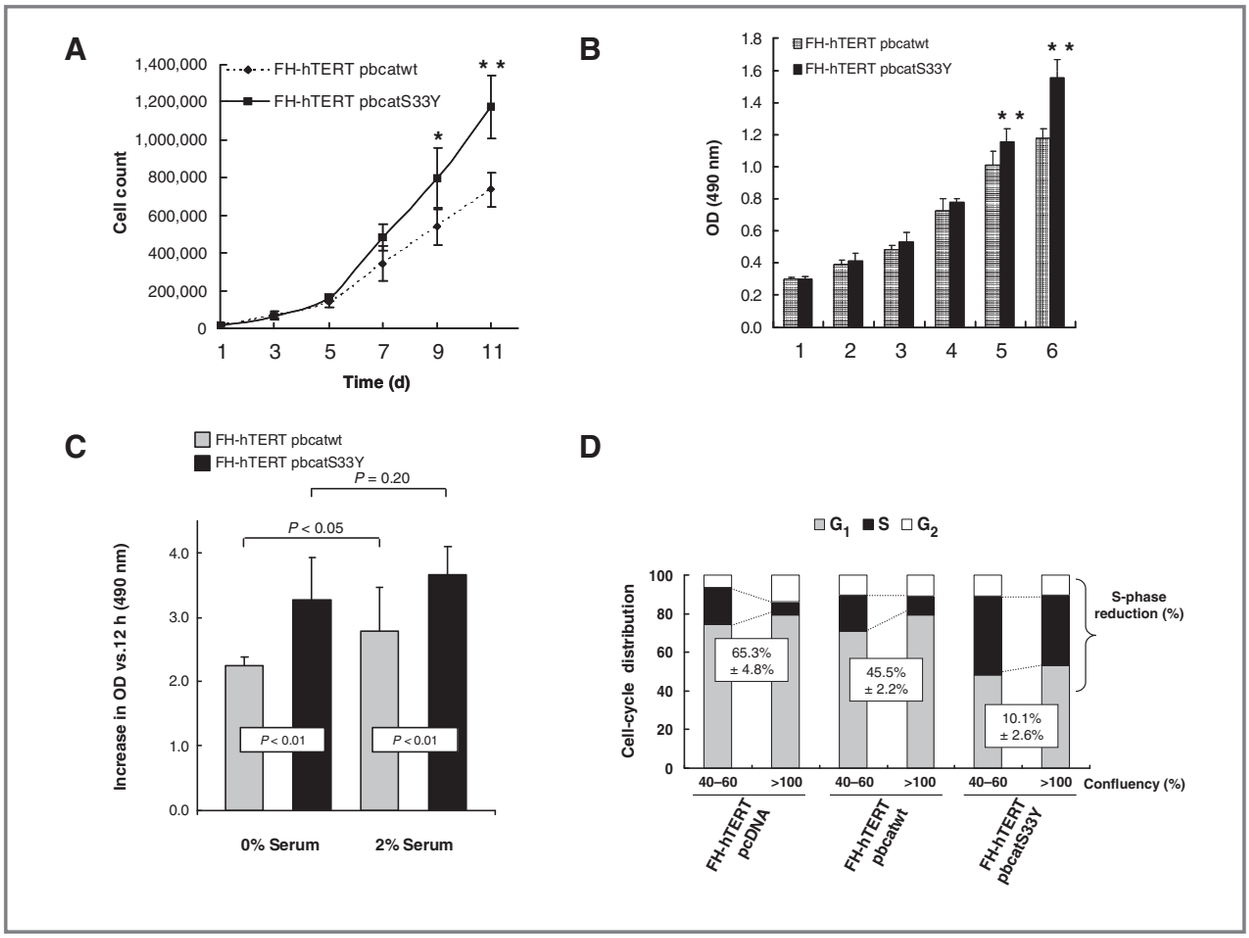

Figure 2. Proliferation analyses. A, proliferation was monitored by serial cell counts at different time points after seeding. Cell counts were obtained from 4 wells per time point. B, for colorimetric measurements of cell density, 8 wells were analyzed per time point. Depicted are means ± SD (error bars). Activation of β-catenin signaling (FH-hTERT pbcatS33Y) led to a significantly enhanced proliferation (*, $P < 0.05$; **, $P < 0.01$). C, to investigate serum dependence, cells were cultured with 0 or 2% serum. Cell density was determined 72 hours after seeding by colorimetric assay (OD vs. 12 hours). Bar graphs (SD = error bars) represent average OD of 8 wells. D, to determine contact inhibition, cell-cycle profiles of near-confluent (40% to 60%) and superconfluent (>100%) cultures were obtained by flow cytometry. Histograms were analyzed by ModFit to attain S-phase fractions. Bar graphs show cell-cycle distribution and calculated S-phase reduction (in % compared with near-confluent cultures).

FH-hTERT pcDNA, the S-phase fraction was reduced by more than 60% in confluent cultures compared with near-confluent cultures, which shows effective growth inhibition by cell-to-cell contacts. In FH-hTERT pbcatS33Y, contact inhibition was almost completely eliminated, that is, the S-phase fraction was reduced by only 10% (Fig. 2D).

Clones with enhanced β-catenin signaling acquired translocations

Previous cytogenetic investigations showed that FH-hTERT maintained a rather intact karyotype and did not acquire clonal structural chromosomal aberrations in long-term expansion culture (25). In this study, cytogenetic monitoring of FH-hTERT pbcatS33Y revealed acquisition of translocations, which were not observed in FH-hTERT control cells. Employing mFISH, 37 metaphase spreads were analyzed. Nineteen metaphases showed the translocations t (5;19)(q31;p11orq11) and t(10;11)(p13;q21) (Fig. 3A). In addition, nonclonal structural and numerical abnormalities were detected in 25 metaphases. Further analyses based on SNP arrays exposed additional microamplifications and deletions on almost all chromosomes (Fig. 3B). Taken together, these data suggest that FH-hTERT pbcatS33Y at least maintained the ability to proliferate despite chromosomal instability and potentially promoted the acquisition of structural chromosomal abnormalities.

Telomerase and β-catenin support a transformed phenotype

Anchorage-independent growth is an established *in vitro* marker for a malignant phenotype. Interestingly, after a few additional passages in cell culture, FH-hTERT pbcatS33Y developed the ability to generate colonies in soft agar (Table 1). Anchorage-independent growth was not observed

Published OnlineFirst August 1, 2011; DOI: 10.1158/1541-7786.MCR-10-0474

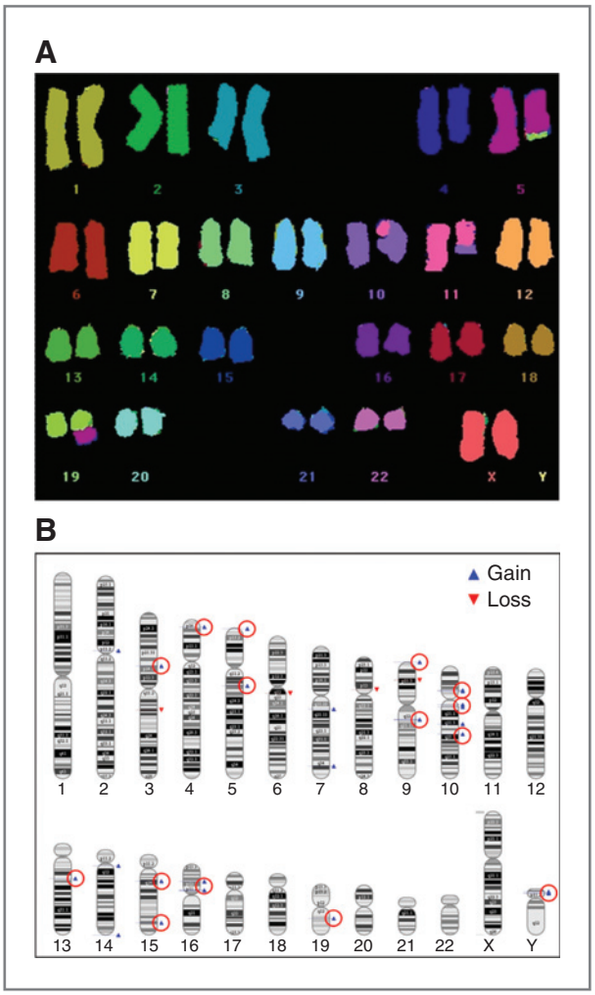

Figure 3. Cytogenetic investigations. A, mFISH showed clonal structural chromosomal aberrations in FH-hTERT pbcatS33Y, shown is a representative karyotype with the translocations t(5;19)(q31;p11orq11) and t(10;11)(p13;q21). B, SNP arrays were conducted to detect microamplifications (gains) and deletions (loss) in DNA samples obtained from FH-hTERT pbcatS33Y in comparison with the HapMap reference and FH-hTERT controls. New gains and losses in FH-hTERT pbcatS33Y are marked (red circle).

in FH-hTERT pcDNA and FH-hTERT pbcatwt. In addition, early passage FH-hTERT (PD 35–40, immediately after bypassing the senescence checkpoint) treated with pbcatS33Y also developed anchorage-independent growth capabilities, however, with a significantly lower frequency (Table 1). To confirm the association between β-catenin activation and anchorage-independent growth, we also scored colony formation in Huh7 cells with and without illegitimate β-catenin activation. In this hepatocellular carcinoma cell line, expression of pbcatS33Y significantly induced colony growth in comparison with control cells. It should be noted that colony formation was observed in malignant Huh7 cells after approximately 2 weeks whereas colonies were seen in FH-hTERT pbcatS33Y only after a significantly longer latency period of 7 weeks (Table 1).

Table 1. Anchorage-independent growth

Cell clone	Colonies up to 2 weeks	Colonies up to 7 weeks
1×10^4 cells/plate		
FH-hTERT pcDNA	0	0
FH-hTERT pbcatwt	0	0
FH-hTERT pbcatS33Y, PD 80–100	0	144 ± 5[b]
FH-hTERT pbcatS33Y, PD 35–40	0	15 ± 4
5×10^3 cells/plate		
Huh7	91 ± 12	NA
Huh7 pbcatS33Y	167 ± 41[a]	NA

NOTE: Values are means ± SD.
Abbreviation: NA, not applicable.
[a]*P* versus Huh7 < 0.05.
[b]*P* versus PD (35–40) < 0.001.

As gold standard proof for a transformed phenotype, FH-hTERT pbcatS33Y were transplanted subcutaneously into athymic nude mice. We transplanted Huh7 cells as a positive control. Tumor formation data are listed in Table 2. As expected and as previously shown (26), no tumor formation was detected in mice transplanted with control cells and FH-hTERT pbcatwt during a 1-year observation period. However, after a mean latency period of 19.0 ± 3.0 weeks, tumors formed in all FH-hTERT pbcatS33Y transplantation sites (Fig. 4A). Notably again, tumors formed with a significantly longer latency period compared with mice transplanted with Huh7 cells (Table 2). As further support for the oncogenic potential of forced β-catenin activation, tumor formation was also significantly accelerated in Huh7 cells following expression of pbcatS33Y (3.4 ± 0.9 weeks vs. 7.7 ± 2.6 weeks, $P < 0.001$). Huh7 pbcatS33Y cells reached a tumor size of approximately 0.8 cm^3 in less than 3 weeks. In contrast, FH-hTERT pbcatS33Y tumors grew less aggressively (Fig. 4B). PCR genotyping and immunofluorescence employing a human-specific antibody for the nuclear antigen SP-100 clearly established that the observed tumors in mice transplanted with FH-hTERT pbcatS33Y and secondary cell lines derived from these tumors originate from transplanted human cells (Supplementary Figs. S2 and 3).

Short-term expansion of FH-hTERT pbcatS33Y was not influenced by telomerase inhibition via RNAi-mediated knockdown of *hTERC* and *hTERT* (Supplementary Fig. S4). In this experiment, cells were not expanded until the telomere-dependent senescence checkpoint.

Cancer pathway profiling in derived tumors

To characterize the transformation process from immortalized cells to premalignant cells and finally established tumors, we profiled various cancer pathways employing qPCR array technology. The analyses revealed

Published OnlineFirst August 1, 2011; DOI: 10.1158/1541-7786.MCR-10-0474

Table 2. Tumor formation in athymic nude mice

Cell clone	Transplantation sites (*n*)	Tumors, *n* (%)	Latency, wk
FH-hTERT pcDNA	10	0	NA
FH-hTERT pbcatwt	8	0	NA
FH-hTERT pbcatS33Y	16	16 (100)	19.0 ± 3.0[a]
Huh7	8	7 (87.5)	7.7 ± 2.6
Huh7 pbcatS33Y	10	9 (90)	3.4 ± 0.9[a]

NOTE: Values are means ± SD.
[a]*P* versus Huh7 < 0.001.

the differential expression of various cell-cycle regulators involved in the execution of senescence, apoptosis, and DNA damage response programs. For instance, *CDKN1A* (p21) was downregulated in FH-hTERT pbcatS33Y and displayed a further decrease in FH-hTERT pbcatS33Y–derived tumors. In contrast, we observed an upregulation for *CHEK2* (*RAD53*), *RB1*, the gene coding for the retinoblastoma protein, and the transcription factor *E2F1*, in FH-hTERT pbcatS33Y as well as in derived tumors. Expression of the tumor suppressor *TP53* was not significantly altered in investigated tumor samples. However, S100 calcium-binding protein A4 (*S100A4*), a strong plasminogen activator inhibitor, was upregulated by more than 2 log levels in 3 of 4 assessed tumors (Fig. 5A). The integrins *ITGA1*, *ITGA2*, and *ITGA3* were all decreased in derived tumors whereas the integrin *ITGA4* (also known as CD49d) was 10-fold upregulated in FH-hTERT pbactS33Y and in derived tumors (Fig. 5B). Furthermore, the matrix metalloproteinase 1 (*MMP1*) displayed elevated and the plasminogen activator inhibitor *SERPINE1* decreased expression levels in FH-hTERT pbcatS33Y and in derived tumors. Urokinase-type plasminogen activator (*PLAU*) also plays a major role in cancer invasion and was induced by β-catenin activation in our model system with high expression in most investigated tumors (Fig. 5C). Interestingly, *VEGFA* was not elevated in the majority of derived tumors. However, we observed an upregulation of *IGF* in samples with low *VEGFA* and a strong suppression of thrombospondin 1 (*THBS1*), a strong inhibitor of neovascularization and tumorigenesis (Fig. 5D).

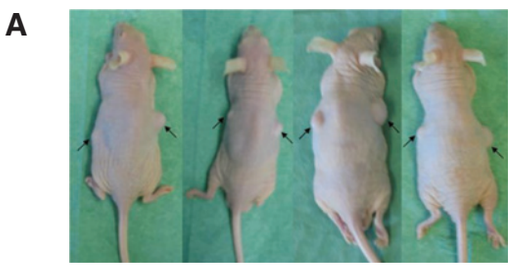

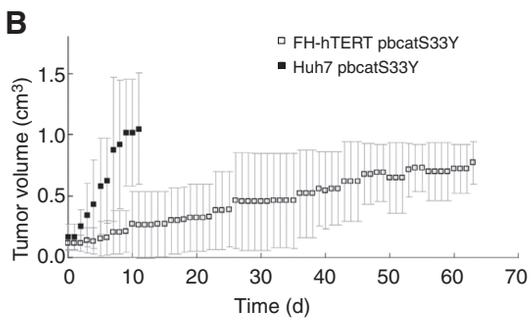

Figure 4. Tumor formation. A, FH-hTERT pbcatS33Y cells were transplanted subcutaneously into the dorsal flanks of athymic nude mice. Tumor volumes were measured 3 times per week using a caliper. The photographs show representative mice with tumor growth observed in all transplantation sites. B, tumor growth curves for transplanted Huh7 pbcatS33Y and FH-hTERT pbcatS33Y cells were generated from caliper measurements. Day 0 was defined as first day of detected tumor growth to adjust for different latency periods until tumor formation. Mice with a tumor volume greater than 0.8 cm^3 were sacrificed.

Discussion

The development and progression of cancer is accompanied by complex changes in gene expression patterns and multiple genetic alterations. To this regard, genome-wide cDNA microarray studies have been successfully used to identify differences in gene expression between hepatocellular carcinoma and the surrounding nonmalignant liver tissue (29, 30). Nevertheless, on the basis of hepatocellular carcinoma molecular signatures, it is currently not possible to attribute functional (cancer driving) properties to individual genetic hits or expression clusters and to define a sequential hierarchy for the identified molecular changes. In contrast to descriptive genome-wide studies evaluating clinical samples, our cell culture model offers the possibility to study functional consequences of distinct genetic alterations. We have previously shown that telomerase activation confers immortality (unlimited replicative potential) without inducing a transformed phenotype (25). The current study provides, for the first time in an untransformed human model system, evidence that an aberrant activation of Wnt/β-catenin signaling accelerates proliferation with reduced serum dependence. Therefore, β-catenin activation further promotes the transformation process and, by establishing self-sufficiency in growth signals and eliminating contact inhibition, increases the risk for malignant transformation. Moreover, these growth-accelerating functional consequences of Wnt/β-catenin activation result in a permissive cellular phenotype characterized by sustained proliferation despite the acquisition (or possibly even promotion) of structural cytogenetic changes. In our study, cytogenetic monitoring revealed the development of persisting translocations in β-catenin–activated cells, as shown by their clonal

Published OnlineFirst August 1, 2011; DOI: 10.1158/1541-7786.MCR-10-0474

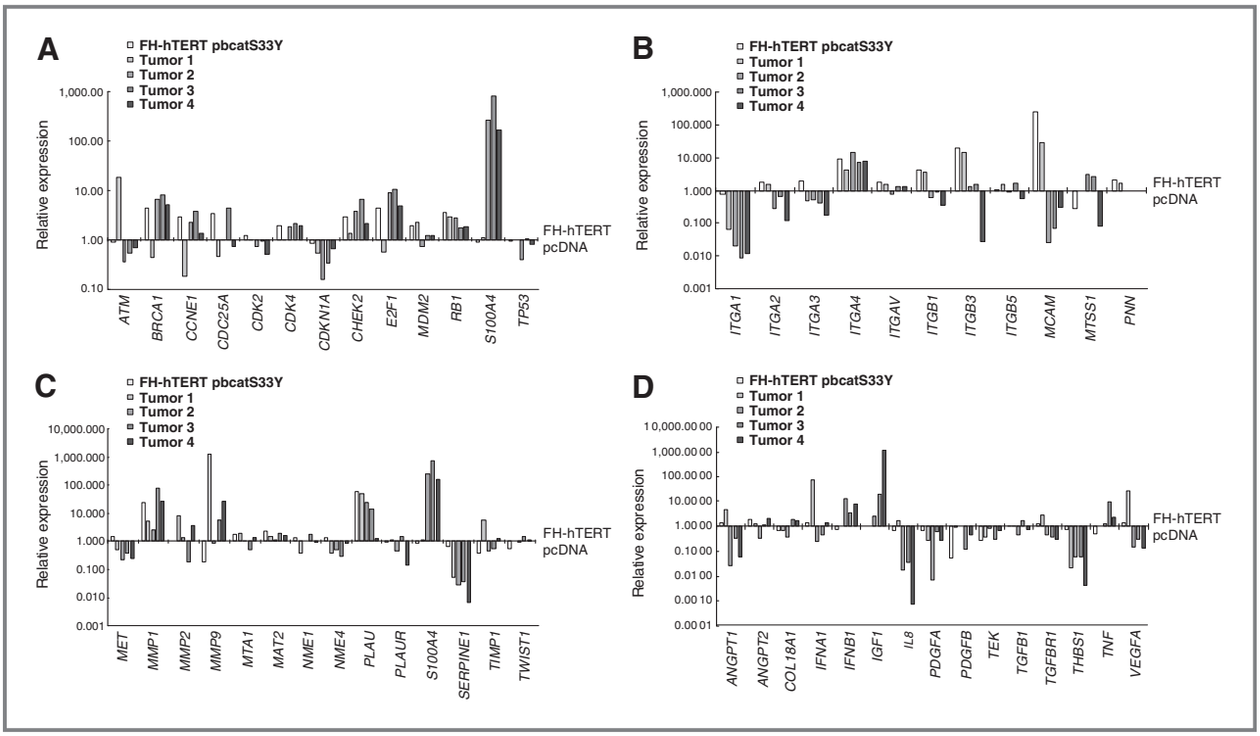

Figure 5. Cancer pathway profiling. Expression studies were conducted in FH-hTERT pbactS33Y and samples from 4 different tumors employing qPCR array technology profiling genes involved in tumorigenesis. Normalized expression levels were compared with FH-hTERT pcDNA as calibrator (expression level = 1). Assessed genes are part of biological pathways involved in the following: A, cell-cycle control and DNA damage repair; B, adhesion; C, invasion and metastasis; and D, angiogenesis.

appearance. This has not been observed in telomerase-immortalized clones without forced β-catenin signaling during long-term expansion culture (25) and thus indicates that additional mutation events are tolerated in telomerase- and β-catenin–positive human fetal hepatocytes and seem to be required for the establishment of a full cancer phenotype. As proof of principle for the driving role of β-catenin activation in hepatocarcinogenesis, only a few passages in cell culture resulted in a transformed phenotype with anchorage-independent growth and tumor formation in athymic nude mice.

Although only 20% to 30% of hepatocellular carcinoma samples exhibit a direct activation of Wnt/β-catenin signaling induced by mutations in the *APC* or *CTNNB1*, 70% of all cases show upregulation of the pathway (19). As additional support to the already known involvement of β-catenin signaling in proliferation and survival of tumor cells, it has recently been shown that in the absence of nuclear factor kappaB (NF-κB) activation, resistance towards apoptosis in premalignant hepatocytes was sustained by an aberrant β-catenin signaling (31). Clearly, animal models suggest that aberrant β-catenin signaling is by itself not sufficient to induce malignancy. To this regard, Harada and colleagues constructed a mouse strain [*Catnb*$^{lox(ex3)}$] containing a mutant β-catenin allele with exon 3 sandwiched by loxP sites. Cre-mediated deletion of β-catenin phosphorylation sites, resulting in pathway activation, caused numerous adenomatous polyps in the intestines but no neoplastic foci in the liver (32). In line with this finding, patients with *APC* mutations do not seem to be characterized by an increased frequency of hepatocellular carcinoma. Taken together, these and our observations corroborate that in addition to telomerase and β-catenin activation, further oncogenic mutations are required to establish a full cancer phenotype. On the other hand, activation of β-catenin signaling provided an additional proliferative advantage during *c-Myc/E2F1*–driven hepatocarcinogenesis (33). This proliferative advantage of immortalized cells with forced β-catenin pathway activation has been functionally confirmed for human liver cells in our model system. To this regard, RNAi experiments in our cell clones established that hTERT and telomerase activity are not required to maintain proliferation in transformed cells. It still needs to be clarified how frequently immortalized cells with forced β-catenin activation escape telomere-dependent cell-cycle arrest following telomerase inhibition.

Intriguingly, patients with hepatocellular carcinoma and β-catenin mutations frequently lack any significant fibrosis or cirrhosis (34). In addition, recent publications report induction of Wnt/β-catenin signaling by the hepatitis B virus X protein (35) and the core protein of the hepatitis C virus (36) as potential mechanism driving hepatocarcinogenesis in a noncirrhotic liver. These reports and our observation

Published OnlineFirst August 1, 2011; DOI: 10.1158/1541-7786.MCR-10-0474

that β-catenin activation induces a cancer-permissive phenotype in telomerase-immortalized cells, strongly support the notion that β-catenin dysregulation is one of the critical hits in the development of hepatocellular carcinoma. In the light of these findings, the proposed therapeutic application of β-catenin activation to promote progenitor cell–driven liver regeneration in hepatic failure or in small-for-size grafts following liver transplantation (34) should be explored with great caution.

In tumors derived form β-catenin–active telomerase-immortalized cells, cancer pathway profiling revealed upregulation of *VEGFA* or *IGFI*, *MMP1*, and *PLAU*. MMPs play an important role in cancer cell invasion by degrading extracellular matrices. For instance, hepatocellular carcinoma cells constitutively expressing MMPs can promote cells to invade through matrix gel *in vitro* and this MMP-dependent invasion is increased in response to hepatocyte growth factor and is blocked by MMP inhibitors (37). Moreover, the plasminogen activator *PLAU* was activated by β-catenin in our model system. Interestingly, in all investigated tumors, we also observed a 2 log level suppression of *SERPINE1*, one of the major plasminogen activator inhibitors. A recent analysis confirmed that *PLAU* downregulation leads to decreased migration and proliferation abilities of hepatocellular carcinoma cells (38). Interestingly, *VEGFA* was not upregulated in all investigated tumors. Alternatively, angiogenesis in our model system seems to be mediated by *IGFI* and suppression of *THBS1*. To this regard, a screening of clinical samples revealed a correlation between *THBS1* expression and tumor invasiveness and progression in hepatocellular carcinoma (39).

In summary, our results recapitulate multistep hepatocarcinogenesis driven by telomerase activation and Wnt/β-catenin signaling. Unlimited proliferation conferred by telomere stabilization is an early requirement during the transformation process, however, not sufficient to induce a malignant phenotype. Additional β-catenin activation induces cancer cell characteristics and further promotes the transition from immortalization to malignant transformation. Transformation in β-catenin–positive hTERT-immortalized cells is associated with the acquisition of translocations, microamplifications, and deletions.

Disclosure of Potential Conflicts of Interest

No potential conflicts of interest were disclosed.

Acknowledgments

The authors thank H. Clevers (Hubrecht Laboratory), R.T. Moon (Howard Hughes Medical Institute), and H. Will (Heinrich-Pette-Institute) for providing plasmids and antibodies as listed. The authors are grateful for bioinformatics support provided by T. Streichert and B. Otto (Array Service Center of the Department of Clinical Chemistry, University Medical Center Hamburg-Eppendorf).

Grant Support

The work was supported by Deutsche Forschungsgemeinschaft (WE2903/1-3 and SFB 841).

The costs of publication of this article were defrayed in part by the payment of page charges. This article must therefore be hereby marked *advertisement* in accordance with 18 U.S.C. Section 1734 solely to indicate this fact.

Received October 21, 2010; revised June 23, 2011; accepted July 26, 2011; published OnlineFirst August 1, 2011.

References

1. Hussain K, El-Serag HB. Epidemiology, screening, diagnosis and treatment of hepatocellular carcinoma. Minerva Gastroenterol Dietol 2009;55:123–38.
2. Altekruse SF, McGlynn KA, Reichman ME. Hepatocellular carcinoma incidence, mortality, and survival trends in the United States from 1975 to 2005. J Clin Oncol 2009;27:1485–91.
3. Shay JW, Bacchetti S. A survey of telomerase activity in human cancer. Eur J Cancer 1997;33:787–91.
4. Greider CW, Blackburn EH. Identification of a specific telomere terminal transferase activity in Tetrahymena extracts. Cell 1985;43:405–13.
5. Greider CW. Telomeres. Curr Opin Cell Biol 1991;3:444–51.
6. Shay JW, Pereira-Smith OM, Wright WE. A role for both RB and p53 in the regulation of human cellular senescence. Exp Cell Res 1991;196:33–9.
7. Oh BK, Jo CK, Park C, Kim K, Jung LW, Han KH, et al. Telomere shortening and telomerase reactivation in dysplastic nodules of human hepatocarcinogenesis. J Hepatol 2003;39:786–92.
8. Oh BK, Kim YJ, Park C, Park YN. Up-regulation of telomere-binding proteins, TRF1, TRF2, and TIN2 is related to telomere shortening during human multistep hepatocarcinogenesis. Am J Pathol 2005;166:73–80.
9. Takaishi H, Kitamoto M, Takahashi S, Aikata H, Kawakami Y, Nakanishi T, et al. Precancerous hepatic nodules had significant levels of telomerase activity determined by sensitive quantitation using a hybridization protection assay. Cancer 2000;88:312–7.
10. Hytiroglou P, Kotoula V, Thung SN, Tsokos M, Fiel MI, Papadimitriou CS. Telomerase activity in precancerous hepatic nodules. Cancer 1998;82:1831–8.
11. Kojima H, Yokosuka O, Imazeki F, Saisho H, Omata M. Telomerase activity and telomere length in hepatocellular carcinoma and chronic liver disease. Gastroenterology 1997;112:493–500.
12. Komine F, Shimojima M, Moriyama M, Amaki S, Uchida T, Arakawa Y. Telomerase activity of needle-biopsied liver samples: its usefulness for diagnosis and judgement of efficacy of treatment of small hepatocellular carcinoma. J Hepatol 2000;32:235–41.
13. Hanahan D, Weinberg RA. The hallmarks of cancer. Cell 2000;100:57–70.
14. Takigawa Y, Brown AM. Wnt signaling in liver cancer. Curr Drug Targets 2008;9:1013–24.
15. Tan X, Yuan Y, Zeng G, Apte U, Thompson MD, Cieply B, et al. Beta-catenin deletion in hepatoblasts disrupts hepatic morphogenesis and survival during mouse development. Hepatology 2008;47:1667–79.
16. Thompson MD, Monga SP. WNT/beta-catenin signaling in liver health and disease. Hepatology 2007;45:1298–305.
17. Apte U, Thompson MD, Cui S, Liu B, Cieply B, Monga SP. Wnt/beta-catenin signaling mediates oval cell response in rodents. Hepatology 2008;47:288–95.
18. Hu M, Kurobe M, Jeong YJ, Fuerer C, Ghole S, Nusse R, et al. Wnt/beta-catenin signaling in murine hepatic transit amplifying progenitor cells. Gastroenterology 2007;133:1579–91.
19. Lee HC, Kim M, Wands JR. Wnt/Frizzled signaling in hepatocellular carcinoma. Front Biosci 2006;11:1901–15.
20. Lustig B, Behrens J. The Wnt signaling pathway and its role in tumor development. J Cancer Res Clin Oncol 2003;129:199–221.

Published OnlineFirst August 1, 2011; DOI: 10.1158/1541-7786.MCR-10-0474

21. Kinzler KW, Vogelstein B. Lessons from hereditary colorectal cancer. Cell 1996;87:159–70.
22. Morin PJ, Sparks AB, Korinek V, Barker N, Clevers H, Vogelstein B, et al. Activation of beta-catenin-Tcf signaling in colon cancer by mutations in beta-catenin or APC. Science 1997;275:1787–90.
23. Firestein R, Bass AJ, Kim SY, Dunn IF, Silver SJ, Guney I, et al. CDK8 is a colorectal cancer oncogene that regulates beta-catenin activity. Nature 2008;455:547–51.
24. Laurent-Puig P, Zucman-Rossi J. Genetics of hepatocellular tumors. Oncogene 2006;25:3778–86.
25. Haker B, Fuchs S, Dierlamm J, Brummendorf TH, Wege H. Absence of oncogenic transformation despite acquisition of cytogenetic aberrations in long-term cultured telomerase-immortalized human fetal hepatocytes. Cancer Lett 2007;256:120–7.
26. Wege H, Le HT, Chui MS, Liu L, Wu J, Giri R, et al. Telomerase reconstitution immortalizes human fetal hepatocytes without disrupting their differentiation potential. Gastroenterology 2003;124:432–44.
27. Fleige S, Walf V, Huch S, Prgomet C, Sehm J, Pfaffl MW. Comparison of relative mRNA quantification models and the impact of RNA integrity in quantitative real-time RT-PCR. Biotechnol Lett 2006;28:1601–13.
28. Wege H, Muller A, Muller L, Petri S, Petersen J, Hillert C. Regeneration in pig livers by compensatory hyperplasia induces high levels of telomerase activity. Comp Hepatol 2007;6:6.
29. Hoshida Y, Villanueva A, Llovet JM. Molecular profiling to predict hepatocellular carcinoma outcome. Expert Rev Gastroenterol Hepatol 2009;3:101–3.
30. Thorgeirsson SS, Lee JS, Grisham JW. Functional genomics of hepatocellular carcinoma. Hepatology 2006;43:S145–50.
31. Gotschel F, Kern C, Lang S, Sparna T, Markmann C, Schwager J, et al. Inhibition of GSK3 differentially modulates NF-kappaB, CREB, AP-1 and beta-catenin signaling in hepatocytes, but fails to promote TNF-alpha-induced apoptosis. Exp Cell Res 2008;314:1351–66.
32. Harada N, Miyoshi H, Murai N, Oshima H, Tamai Y, Oshima M, et al. Lack of tumorigenesis in the mouse liver after adenovirus-mediated expression of a dominant stable mutant of beta-catenin. Cancer Res 2002;62:1971–7.
33. Calvisi DF, Conner EA, Ladu S, Lemmer ER, Factor VM, Thorgeirsson SS. Activation of the canonical Wnt/beta-catenin pathway confers growth advantages in c-Myc/E2F1 transgenic mouse model of liver cancer. J Hepatol 2005;42:842–9.
34. Nejak-Bowen KN, Monga SP. Beta-catenin signaling, liver regeneration and hepatocellular cancer: sorting the good from the bad. Semin Cancer Biol 2011;21:44–58.
35. Keng VW, Tschida BR, Bell JB, Largaespada DA. Modeling hepatitis B virus X-induced hepatocellular carcinoma in mice with the Sleeping Beauty transposon system. Hepatology 2011;53:781–90.
36. Liu J, Wang Z, Tang J, Tang R, Shan X, Zhang W, et al. Hepatitis C virus core protein activates Wnt/beta-catenin signaling through multiple regulation of upstream molecules in the SMMC-7721 cell line. Arch Virol 2011;156:1013–23.
37. Murakami K, Sakukawa R, Ikeda T, Matsuura T, Hasumura S, Nagamori S, et al. Invasiveness of hepatocellular carcinoma cell lines: contribution of membrane-type 1 matrix metalloproteinase. Neoplasia 1999;1:424–30.
38. Salvi A, Sabelli C, Moncini S, Venturin M, Arici B, Riva P, et al. MicroRNA-23b mediates urokinase and c-met downmodulation and a decreased migration of human hepatocellular carcinoma cells. FEBS J 2009;276:2966–82.
39. Poon RT, Chung KK, Cheung ST, Lau CP, Tong SW, Leung KL, et al. Clinical significance of thrombospondin 1 expression in hepatocellular carcinoma. Clin Cancer Res 2004;10:4150–7.

Published OnlineFirst August 1, 2011; DOI: 10.1158/1541-7786.MCR-10-0474

Molecular Cancer Research

Forced Activation of β-Catenin Signaling Supports the Transformation of *hTERT*-Immortalized Human Fetal Hepatocytes

Henning Wege, Denise Heim, Marc Lütgehetmann, et al.

Mol Cancer Res 2011;9:1222-1231. Published OnlineFirst August 1, 2011.